Distributed MPC-based frequency control for multi-area power systems with energy storage

Luwei Yang[*], Tao Liu, David J. Hill

Department of Electrical and Electronic Engineering, The University of Hong Kong, Hong Kong Special Administrative Region, China

A B S T R A C T

This paper proposes a novel distributed model predictive control (DMPC) scheme for frequency regulation of multi-area power systems with substantial renewable power sources and different types of controllable units including synchronous generators, flexible loads and energy storage devices. The frequency regulation task is firstly formulated as a model predictive control (MPC) problem, and then is solved by a distributed projection-based algorithm via peer-to-peer communication. The objectives of the proposed controller are twofold. Firstly, it is to maintain the system frequency and net inter-area power exchanges at their nominal values by optimally adjusting the active powers of controllable units. Secondly, it is to make the system variables such as the bus frequencies, power output/consumption of each control-lable unit, ramping rates of generators and stored energy levels of storage devices meet their operational constraints. Case studies demonstrate the effectiveness of the designed control method.

1. Introduction

The key task to operate a stable multi-area power system is to keep the frequency and net inter-area power exchanges at their nominal values, which is critical for safety of generating equipment, satisfactory performance of electrical loads as well as reliable power delivery [1]. This objective is traditionally achieved by automatic generation control (AGC) via making the power generation of each control area follow its own load demand [2]. However, due to the uncertainty and intermittency of renewable power outputs, the conventional generation-side control paradigm may be inadequate to regulate the frequency of modern power systems with high penetration of renewable energy resources, e.g., wind and solar powers [3]. A possible way to tackle this challenge is to use more fast-acting spinning reserves, which will definitely incur high operation costs.

As alternative remedies, energy storage devices and controllable loads have attracted considerable attention due to their properties such as instantaneous responsiveness, low emissions and distributed availability throughout the grid [4]. Nevertheless, these new devices have their own issues when participating in frequency regulation, e.g., the operations of controllable loads may impose negative impacts on end-users and storage devices are energy constrained. This presents an urgent need for developing effective control schemes to co-ordinate different types of devices for frequency control by fully

considering their respective characteristics.

To achieve this target, various control techniques have been introduced for frequency regulation in the literature, e.g., the proportional-integral control [5], robust control [6], artificial neural network control [7] and self-adaptive control [8] (see [9] and references therein for more examples). However, it has been pointed out in [10] that these control approaches cannot sufficiently deal with the multivariate constraints of a complex power system, such as the ramping constraints of synchronous generators and energy capacity constraints of storage devices. This drawback significantly discounts their anticipated control performance for practical implementations.

Model predictive control (MPC), which determines control actions by solving an optimization problem over a receding finite time horizon, can be a potential solution for this drawback owing to its capability of handling hard constraints in multivariable systems [11]. Some related results by using the MPC-based strategies to regulate the frequency of multi-area power systems with substantial renewable power resources have been reported in the literature (e.g., [10–17]). References [10–12] focus on the design of centralized frequency control algorithms which are vulnerable to single points of failure and may cause a heavy communication burden. Distributed MPC-based frequency controllers have been proposed in [13–17]. However, references [13,14] only consider generation-side frequency control, but neglect the participation of energy storage devices and controllable loads. Further, they treat all

generators in each control area as an equivalent generating unit exhibiting the overall performance, and thus cannot capture the different properties of individual generators. References [15–17] take energy storage devices into account, but do not consider the limits on bus frequency deviations from the nominal value or the issue of keeping the scheduled net inter-area power exchanges which is also a key task for frequency regulation in multi-area power systems.

In view of the abovementioned issues, this paper proposes a distributed model predictive control (DMPC)-based frequency control algorithm for each synchronous generator, controllable load and energy storage unit in a multi-area power system with substantial renewable power sources. The designed controller aims to regulate the system frequency and net tie-line power flows between physically interconnected control areas tightly around their nominal values by optimally adjusting the power outputs/consumptions of all controllable units. Further, it also aims to keep the operational constraints of the system such as the power/ramping limits of generators, power capacity limits of flexible loads, power/energy limits of energy storage devices as well as bus frequency limits satisfied. The designed DMPC-based frequency controller only relies on local information and communication between cyber-connected buses. Therefore, it allows plug-and-play operations, which is desirable for modern power systems to integrate more renewable energy resources.

The remainder of this paper is organized as follows. Section 2 describes the system model. The frequency regulation task is formulated as an MPC problem in Section 3, and a distributed projection-based algorithm is provided in Section 4 to solve the resulting MPC problem. Simulation studies are conducted in Section 5. Finally, Section 6 gives a conclusion remark.

Notations: Denote $\mathbb{R}$, $\mathbb{R}_+$, $\mathbb{Z}_+$ as the sets of real numbers, non-negative real numbers, non-negative integers; $\mathbb{R}^n$, $\mathbb{R}^{m \times n}$ as the n-dimensional real vectors and $(m \times n)$-dimensional real matrices, respectively. Let $\|x\|$ be the Euclidean norm for vector $x \in \mathbb{R}^n$, and define the operator $\|x\|_A$ by $\|x\|_A = \sqrt{x^T A x}$ with symmetric matrix $A \in \mathbb{R}^{n \times n}$. Denote $\text{diag}(a_1, \cdots, a_k)$ as the diagonal matrix whose ith diagonal entry is $a_i \in \mathbb{R}$, and $S_1 \times \cdots \times S_k$ as the Cartesian product of sets $S_i \subset \mathbb{R}^{n_i}$ with $i = 1, \cdots, k$. We denote $0_{m \times n}$ as the $(m \times n)$-dimensional zero matrix, and drop the subscripts of the matrices when they are obvious in the context. The notation $\text{P}_S(\xi) = \arg\min_{\eta \in S} \|\xi - \eta\|$ represents the projection of vector $\xi \in \mathbb{R}^n$ onto a closed convex set $S \subset \mathbb{R}^n$, and $\text{C}_S(\xi) = \{\nu \in \mathbb{R}^n | \text{P}_S(\nu + \xi) = \xi\}$ denotes the normal cone of S at ξ.

2. Model description

Consider a power transmission network with n buses and τ control areas, whose index sets are defined by $\mathcal{N} = \{1, \cdots, n\}$ and $\mathcal{T} = \{1, \cdots, \tau\}$, respectively. We assume that the power network is connected, and satisfies the following assumptions that are well-justified for real-world transmission networks:

(i) The system frequency is mainly affected by active power flows, and impacts from reactive power flows are neglected;
(ii) Transmission lines are lossless and characterised by their susceptance $B_{ij} = B_{ji} \geq 0$.
(iii) Bus voltage magnitudes $|V_i|$ are fixed for all $i \in \mathcal{N}$;

To describe the dynamics of the power network, we adopt the nonlinear structure-preserving model proposed in [18], and introduce the second-order turbine-governor dynamics into the model. We partition the buses into n_g generator buses and n_l load buses, whose index sets are defined by $\mathcal{N}_{\mathcal{G}} = \{1, \cdots, n_g\}$, and $\mathcal{N}_{\mathcal{L}} = \{n_g + 1, \cdots, n\}$, respectively. Thus, we have $n = n_g + n_l$, and $\mathcal{N} = \mathcal{N}_{\mathcal{G}} \cup \mathcal{N}_{\mathcal{L}}$. Further, we assume all load buses have a frequency-dependent load, and can also be equipped with at least one device such as a renewable generating unit, controllable load, frequency-insensitive non-dispatchable load and energy storage unit, or be without any additional device. We let $\mathcal{N}_C$, $\mathcal{N}_{\mathcal{E}}$ be

the index sets of buses with flexible loads and storage units, respectively. If bus i has both controllable loads and energy storage devices, then $i \in \mathcal{N}_C \cap \mathcal{N}_{\mathcal{E}} \neq \varnothing$.

For each bus $i \in \mathcal{N}$, let ω_i, p_{b_i} be the local frequency deviation from its nominal value and net power flow out of bus i, respectively. For each generator bus let δ_i be the power angle with respect to a synchronously rotating reference; P_{m_i}, P_{v_i}, P_{g_i} be the mechanical power input, governor valve position and load reference set-point; and D_i, M_i, T_{m_i}, T_{v_i}, R_i be the damping coefficient, rotational inertia, governor time constant, turbine time constant and droop-control gain, respectively. For each load bus $i \in \mathcal{N}_{\mathcal{L}}$, let D_i denote the load-frequency sensitive coefficient; δ_i be the bus voltage phase angle; r_i be the local net demand, i.e., frequency-insensitive uncontrollable load minus renewable generation; p_{l_i} be the power consumed by the controllable load; p_{c_i}, p_{d_i} (η_{c_i}, η_{d_i}) be the charging and discharging powers (efficiencies) of the energy storage device, respectively; and e_i be the stored energy level of the storage unit. Then, the system model of the power network is given as follows

$$
\begin{aligned}
\dot{\delta}_i &= \omega_i, \ i \in \mathcal{N} \\
M_i \dot{\omega}_i &= -D_i \omega_i + p_{m_i} - p_{b_i}, \ i \in \mathcal{N}_{\mathcal{G}} \\
T_{m_i} \dot{p}_{m_i} &= -p_{m_i} + p_{v_i}, \ i \in \mathcal{N}_{\mathcal{G}} \\
T_{v_i} \dot{p}_{v_i} &= -\frac{1}{R_i} \omega_i - p_{v_i} + p_{g_i}, \ i \in \mathcal{N}_{\mathcal{G}} \\
D_i \omega_i &= -r_i - p_{l_i} - p_{c_i} + p_{d_i} - p_{b_i}, \ i \in \mathcal{N}_{\mathcal{L}} \\
\dot{e}_i &= \eta_{c_i} p_{c_i} - \frac{1}{\eta_{d_i}} p_{d_i}, \ i \in \mathcal{N}_{\mathcal{L}} \\
p_{b_i} &= \sum_{j \in \mathcal{N}_i} |V_i||V_j| B_{ij} \sin(\delta_i - \delta_j), \ i \in \mathcal{N}
\end{aligned}
\tag{1}
$$

where for bus $i \in \mathcal{N}_{\mathcal{L}} \setminus \mathcal{N}_C$, i.e., load bus i has no controllable load, $p_{l_i} = 0$; for bus $i \in \mathcal{N}_{\mathcal{L}} \setminus \mathcal{N}_{\mathcal{E}}$, i.e., load bus i has no energy storage unit, $e_i = p_{c_i} = p_{d_i} = \eta_{c_i} = \frac{1}{\eta_{d_i}} = 0$; and $\mathcal{N}_i$ is the index set of buses that are connected with bus i through transmission lines. For generator bus $i \in \mathcal{N}_{\mathcal{G}}$, let $x_i = (\delta_i, \omega_i, p_{m_i}, p_{v_i})^T$, $y_i = p_{b_i}$, $u_i = p_{g_i}$. Further, for load bus $i \in \mathcal{N}_{\mathcal{L}}$, let $x_i = (\delta_i, e_i)^T$, $y_i = (\omega_i, p_{b_i})^T$, $u_i = (p_{l_i}, p_{c_i}, p_{d_i})^T$. Then, the state-space representation of (1) can be expressed as

$$
\dot{x}_i = f_i(x_i, x_j, y_i, u_i)
\tag{2a}
$$

$$
0 = g_i(x_i, x_j, y_i, u_i, r_i)
\tag{2b}
$$

where x_j is the state variable of bus $j \in \mathcal{N}_i$.

3. MPC problem formulation

The control target of this paper is to develop a DMPC-based frequency control scheme for system (2), which can regulate the frequency and net inter-area power exchanges close to their nominal values, and optimally coordinate the power produced by synchronous generators, power drawn by controllable loads and power charged/discharged by energy storage devices while respecting the operational constraints of the system.

To achieve this target, at each sampling instant $t = hT_o$, $h \in \mathbb{Z}_+$, with T_o being the constant sampling period, the DMPC-based frequency controller to be designed uses the current system conditions, forecast net demand profiles over a finite time horizon and linear discrete-time model given below to predict the future behaviours of system (2)

$$
\begin{aligned}
\Delta x_i[k+1] &= \mathcal{A}_{ii}(hT_o) \Delta x_i[k] + \sum_{j \in \mathcal{N}_i} \mathcal{A}_{ij}(hT_o) \Delta x_j[k] \\
&\quad + \mathcal{B}_i(hT_o) \Delta y_i[k] + C_i(hT_o) \Delta u_i[k] \\
0 &= \mathcal{D}_{ii}(hT_o) \Delta x_i[k] + \sum_{j \in \mathcal{N}_i} \mathcal{D}_{ij}(hT_o) \Delta x_j[k] \\
&\quad + \mathcal{E}_i(hT_o) \Delta y_i[k] + \mathcal{F}_i(hT_o) \Delta u_i[k] + \mathcal{G}_i(hT_o) \Delta r_i[k]
\end{aligned}
\tag{3}
$$

where $k = 0, 1, \cdots, n_p - 1$ is the discrete-time step index with n_p being the total prediction step in the prediction window $t \in [hT_o, (h + n_p)T_o)$; $\Delta x_i[k], \Delta y_i[k], \Delta u_i[k], \Delta r_i[k], i \in \mathcal{N}$, are the deviations at step k from the values of $x_i(hT_o)$, $y_i(hT_o)$, $u_i^-(hT_o)$, $r_i(hT_o)$ with $u_i^-(hT_o) = p_{g_i}^-(hT_o)$, $i \in \mathcal{N}_{\mathcal{G}}$ and $u_i^-(hT_o) = (p_{l_i}^-(hT_o), p_{c_i}^-(hT_o), p_{d_i}^-(hT_o))^T$, $i \in \mathcal{N}_{\mathcal{L}}$ being the

control input that bus i currently employs, i.e., right before the prediction starts at $t = hT_o$; and $\mathcal{A}_{ii}(hT_o) - \mathcal{G}_i(hT_o)$ are the system matrices updated at $t = hT_o$. For notational brevity, we will simply denote $\mathcal{A}_{ii}(hT_o) - \mathcal{G}_i(hT_o)$ as $\mathcal{A}_{h_i} - \mathcal{G}_{h_i}$ in the rest of the paper. At each $t = hT_o$, model (3) serves as the predictor of (2) over the prediction window $t \in [hT_o, (h + n_p)T_o)$ and is obtained through a standard process in control theory, i.e., firstly linearize system (2) at its current operating point, and then discretize the derived linearized model with the sampling period T_o. For details of linearization and discretization of a dynamic system, please refer to [10,19], respectively.

Based on the prediction from (3), at each sampling instant $t = hT_o$, the DMPC-based frequency control algorithm solves an MPC problem with respect to frequency regulation over the prediction window $t \in [hT_o, (h + n_p)T_o)$, and only applies the first derived control sequence $\Delta u_i[0]$ to compute the new control signal, i.e., $\Delta u_i[0] + u_i^-(hT_o)$, for dispatching the controllable units at bus $i \in \mathcal{N}$. This process is repeated for the next time step $t = (h + 1)T_o$ by using the latest available information pertaining to the forecast renewable generation and load demand profiles. In particular, at $t = hT_o$, the MPC problem is formulated as follows

$$
\min \sum_{k \in \mathcal{K}} \left(\sum_{i \in \mathcal{N}_G} (f_{\omega_i}(\Delta \omega_i[k + 1]) + f_{m_i}(\Delta p_{m_i}[k + 1])) + \sum_{i \in \mathcal{N}_L} (f_{\omega_i}(\Delta \omega_i[k]) + f_{cd_i}(\Delta p_{c_i}[k], \Delta p_{d_i}[k]) + f_{l_i}(\Delta p_{l_i}[k])) + \sum_{s \in \mathcal{T}} f_{tie_s}\left(\Delta p_{tie_s}[k] \right) \right)
$$

s.t. Equation (3), $\forall i \in \mathcal{N}$ (4a)

$\underline{\omega}_i \leq \Delta \omega_i[k + 1] + \omega_i(hT_o) \leq \overline{\omega}_i, \ \forall i \in \mathcal{N}_G$ (4b)

$\underline{\omega}_i \leq \Delta \omega_i[k] + \omega_i(hT_o) \leq \overline{\omega}_i, \ \forall i \in \mathcal{N}_L$ (4c)

$\underline{p}_{m_i} \leq \Delta p_{m_i}[k + 1] + p_{m_i}(hT_o) \leq \overline{p}_{m_i}, \ \forall i \in \mathcal{N}_G$ (4d)

$\underline{r}_{m_i} \leq \Delta p_{m_i}[k + 1] - \Delta p_{m_i}[k] \leq \overline{r}_{m_i}, \ \forall i \in \mathcal{N}_G$ (4e)

$\underline{p}_{l_i} \leq \Delta p_{l_i}[k] + p_{l_i}^-(hT_o) \leq \overline{p}_{l_i}, \ \forall i \in \mathcal{N}_L$ (4f)

$0 \leq \Delta p_{c_i}[k] + p_{c_i}^-(hT_o) \leq \overline{p}_{c_i}, \ \forall i \in \mathcal{N}_L$ (4g)

$0 \leq \Delta p_{d_i}[k] + p_{d_i}^-(hT_o) \leq \overline{p}_{d_i}, \ \forall i \in \mathcal{N}_L$ (4h)

$0 = (\Delta p_{c_i}[k] + p_{c_i}^-(hT_o))(\Delta p_{d_i}[k] + p_{d_i}^-(hT_o)), \ \forall i \in \mathcal{N}_L$ (4i)

$\underline{e}_i \leq \Delta e_i[k + 1] + e_i(hT_o) \leq \overline{e}_i, \ \forall i \in \mathcal{N}_L$ (4j)

$\Delta p_{tie_s}[k] = \sum_{i \in \mathcal{N}_s} \Delta p_{b_i}[k], \ \forall s \in \mathcal{T}$,   (4k)

$\forall k \in \mathcal{K}$, where $\mathcal{K} = \{0, 1, \cdots, n_p - 1\}$ is the index set of the discrete-time steps in each prediction window; $\mathcal{N}_s$ is the index set of buses within the sth control area, $s \in \mathcal{T}$; $\Delta p_{tie_s}[k]$ is the predicted net tie-line power deviation of the sth control area at step k from its current value $p_{tie_s}(hT_o) = \sum_{i \in \mathcal{N}_s} p_{b_i}(hT_o)$. The functions $f_{\omega_i}(\Delta \omega_i[k])$ and $f_{tie_s}(\Delta p_{tie_s}[k])$ are quadratic penalty terms for mismatches of bus frequencies and net inter-area power exchanges from their nominal values, respectively, and are defined by [10]

$$
f_{\omega_i} = \frac{a_{\omega_i}}{2}(\Delta \omega_i[k] + \omega_i(hT_o))^2, \ i \in \mathcal{N}
$$
$$
f_{tie_s} = \frac{a_{tie_s}}{2}(\Delta p_{tie_s}[k] + p_{tie_s}(hT_o) - p_{tie_s}^{ref})^2, \ s \in \mathcal{T}
$$
   (5)

with $a_{\omega_i}, a_{tie_s} > 0$, where $p_{tie_s}^{ref}$ is the scheduled (reference) net tie-line power of the sth control area. For the generator at bus $i \in \mathcal{N}_G$, $f_{m_i}(\Delta p_{m_i}(k))$ is the generation cost at step k; $\underline{p}_{m_i}, \overline{p}_{m_i}$ are the minimum and maximum power outputs; and $\underline{r}_{m_i}, \overline{r}_{m_i}$ are the ramp-down and ramp-up limits, respectively. For the controllable load at bus $i \in \mathcal{N}_C$, $f_{l_i}(\Delta p_{l_i}(k))$ is the user disutility at step k, and $\underline{p}_{l_i}, \overline{p}_{l_i}$ denote the power capacity limits. Furthermore, for bus $i \in \mathcal{N}_L \backslash \mathcal{N}_C$, i.e., load bus i has no

flexible load, we set $f_{l_i} = \underline{p}_{l_i} = \overline{p}_{l_i} = 0$. For the energy storage device at bus $i \in \mathcal{N}_\mathcal{E}$, $f_{cd_i}(\Delta p_{c_i}[k], \Delta p_{d_i}[k])$ is the operation cost at step k; $\overline{p}_{c_i}, \overline{p}_{d_i}$ are the maximum allowable charging and discharging powers; and $\underline{e}_i, \overline{e}_i$ are the lower and upper bounds on the stored energy, respectively. Moreover, for bus $i \in \mathcal{N}_L \backslash \mathcal{N}_\mathcal{E}$, i.e., load bus i has no storage unit, we set $f_{cd_i} = \overline{p}_{c_i} = \overline{p}_{d_i} = \underline{e}_i = \overline{e}_i = 0$. For any bus $i \in \mathcal{N}$, $\underline{\omega}_i, \overline{\omega}_i$ are the constraints on the local frequency.

With respect to the MPC problem (4), the objective function aims to minimize the total penalty of bus frequency and net inter-area power flow deviations from their nominal values and total operation cost of all controllable units across the whole prediction window $t \in [hT_o, (h + n_p)T_o)$. Constraint (4a), i.e., the linear discrete-time model (3), plays a role as the predictor of the future behaviours of (2). Instead of employing the fixed model linearized at the initial operating point [10,11], the system matrices in (3) are updated at every sampling instant $t = hT_o$ to avoid large prediction errors. Furthermore, using the linearized model as the predictor rather than the original nonlinear one transforms the nonlinear optimization problem to a linear-quadratic programming problem [4], which not only simplifies the computation but also facilitates the distributed solution algorithm design. In addition, by taking full advantage of the accurate (short-term) forecasts of renewable generation and their (long-term) fluctuation tendency in constraint (4a), the MPC problem (4) aims to reach optimal control results not only at present, but also in the long run. Constraints (4b), (4c) are to limit all bus frequencies within their acceptable ranges. Constraints (4d), (4e) are the power capacity limits and ramping limits of generators, respectively. The power consumptions of controllable loads are limited by (4f), and storage charging and discharging powers are respectively bounded by (4g), (4h). Constraint (4i) is to circumvent the simultaneous charge and discharge of energy storage units. Constraint (4j) describes the energy capacity limits of storage devices. Finally, constraint (4k) uses $\Delta p_{tie_s}[k]$ to estimate the net tie-line power of the sth control area at step k.

In this paper, we adopt the standard quadratic generation cost function and user disutility function for each synchronous generator and controllable load as follows [20]

$$
f_{m_i} = \frac{a_{m_i}}{2}(\Delta p_{m_i}[k] + p_{m_i}(hT_o))^2 + b_{m_i}(\Delta p_{m_i}[k] + p_{m_i}(hT_o)) + c_{m_i}, \ i \in \mathcal{N}_G
$$
$$
f_{l_i} = \frac{a_{l_i}}{2}(\Delta p_{l_i}[k] + p_{l_i}^-(hT_o))^2 + b_{l_i}(\Delta p_{l_i}[k] + p_{l_i}^-(hT_o)) + c_{l_i}, \ i \in \mathcal{N}_C
$$
   (6)

where $a_{m_i}, b_{m_i}, c_{m_i}, a_{l_i}, b_{l_i}, c_{l_i} \in \mathbb{R}$ are constants with $a_{m_i} > 0, \forall i \in \mathcal{N}_G$, and $a_{l_i} > 0, \forall i \in \mathcal{N}_C$. In addition, we adopt the following linear function of both charging and discharging powers to describe the operation cost of energy storage units, which is extensively used in energy storage systems [21]

$$
f_{cd_i} = b_{cd_i}(\Delta p_{c_i}[k] + p_{c_i}^-(hT_o) + \Delta p_{d_i}[k] + p_{d_i}^-(hT_o)) + c_{cd_i}, \ i \in \mathcal{N}_\mathcal{E}
$$
   (7)

where $b_{cd_i}, c_{cd_i} \in \mathbb{R}$ are constants with $b_{cd_i} > 0, \forall i \in \mathcal{N}_\mathcal{E}$. As argued in [21], since function (7) is monotonically increasing, it can prevent the charging power $\Delta p_{c_i}[k] + p_{c_i}^-(hT_o)$ and discharging power $\Delta p_{d_i}[k] + p_{d_i}^-(hT_o)$ of each energy storage device from being simultaneously nonzero, which thus implies that all storage units can only operate either in the charge or discharge mode at any time. Therefore, with the selected f_{cd_i} in (7), constraint (4i) can be deleted in the MPC problem (4). For details of the physical meanings of the above cost/disutility functions, please refer to [20,21].

For generator bus $i \in \mathcal{N}_G$, we define sets $\Omega_{x_i} = \mathbb{R} \times [\underline{\omega}_i - \omega_i(hT_o), \overline{\omega}_i - \omega_i(hT_o)]$ $\Omega_{y_i} = \mathbb{R}$, and $\Omega_{u_i} = \mathbb{R}$.

$\times [\underline{p}_{m_i} - p_{m_i}(hT_o), \overline{p}_{m_i} - p_{m_i}(hT_o)] \times \mathbb{R}$,

Further, for load bus $i \in \mathcal{N}_L$, we define sets $\Omega_{x_i} = \mathbb{R} \times [\underline{e}_i - e_i(hT_o), \overline{e}_i - e_i(hT_o)]$,

$\Omega_{y_i} = [\underline{\omega}_i - \omega_i(hT_o), \overline{\omega}_i - \omega_i(hT_o)] \times \mathbb{R}$, and $\Omega_{u_i} = [\underline{p}_{l_i} - p_{l_i}^-(hT_o),$
$\overline{p}_{l_i} - p_{l_i}^-(hT_o)] \times [-p_{c_i}^-(hT_o), \overline{p}_{c_i} - p_{c_i}^-(hT_o)] \times [-p_{d_i}^-(hT_o), \overline{p}_{d_i} - p_{d_i}^-(hT_o)]$.
Then, we can rewrite the MPC problem (4) in the matrix form as follows

$$
\min \sum_{k \in \mathcal{K}} \left(\sum_{i \in \mathcal{N}} (\frac{1}{2} \|\Delta x_i[k+1] + x_i(hT_o)\|_{\mathcal{A}_{x_i}}^2 \right.
$$
$$
+ \frac{1}{2}\|\Delta y_i[k] + y_i(hT_o)\|_{\mathcal{A}_{y_i}}^2 + \frac{1}{2}\|\Delta u_i[k] + u_i^-(hT_o)\|_{\mathcal{A}_{u_i}}^2
$$
$$
+ \mathcal{B}_{x_i}^T(\Delta x_i[k+1] + x_i(hT_o)) + \mathcal{B}_{u_i}^T(\Delta u_i[k] + u_i^-(hT_o))
$$
$$
\left. + C_i) + \sum_{s \in \mathcal{T}} \frac{1}{2}\|\Delta p_{tie_s}[k] + p_{tie_s}(hT_o) - p_{tie_s}^{ref}\|_{\mathcal{A}_{tie_s}}^2 \right)
$$

s.t. Equation (3), $\forall i \in \mathcal{N}$ (8a)

$$
\underline{r}_{m_i} \le \mathcal{J}_{m_i}^T(\Delta x_i[k+1] - \Delta x_i[k]) \le \overline{r}_{m_i}, \quad \forall i \in \mathcal{N} \tag{8b}
$$

$$
\Delta x_i[k+1] \in \Omega_{x_i}, \quad \Delta y_i[k] \in \Omega_{y_i}, \quad \Delta u_i[k] \in \Omega_{u_i}, \quad \forall i \in \mathcal{N} \tag{8c}
$$

$$
\Delta p_{tie_s}[k] = \sum_{i \in \mathcal{N}_s} \mathcal{J}_{b_i}^T \Delta y_i[k], \quad \forall s \in \mathcal{T}, \tag{8d}
$$

$\forall k \in \mathcal{K}$, where $\underline{r}_{m_i} = \overline{r}_{m_i} = 0, \forall i \in \mathcal{N}_{\mathcal{L}}$. The matrices in (8) are defined by

$$
\mathcal{A}_{x_i} = \text{diag}(0, a_{\omega_i}, a_{m_i}, 0), \quad \mathcal{A}_{y_i} = 0, \quad \mathcal{A}_{u_i} = 0,
$$
$$
\mathcal{B}_{x_i} = (0, 0, b_{m_i}, 0)^T, \quad \mathcal{B}_{u_i} = 0, \quad C_i = c_{m_i},
$$
$$
\mathcal{J}_{m_i} = (0, 0, 1, 0)^T, \quad \mathcal{J}_{b_i} = 1, \quad \forall i \in \mathcal{N}_{\mathcal{G}} \tag{9a}
$$

$$
\mathcal{A}_{x_i} = 0_{2 \times 2}, \quad \mathcal{A}_{y_i} = \text{diag}(a_{\omega_i}, 0), \quad \mathcal{A}_{u_i} = \text{diag}(a_{l_i}, 0, 0),
$$
$$
\mathcal{B}_{x_i} = 0_{2 \times 1}, \quad \mathcal{B}_{u_i} = (b_{l_i}, b_{cd_i}, b_{cd_i})^T, \quad C_i = c_{l_i} + c_{cd_i},
$$
$$
\mathcal{J}_{m_i} = 0_{2 \times 1}, \quad \mathcal{J}_{b_i} = (0, 1)^T, \quad \forall i \in \mathcal{N}_{\mathcal{L}} \tag{9b}
$$

$$
\mathcal{A}_{tie_s} = a_{tie_s}, \quad \forall s \in \mathcal{T}. \tag{9c}
$$

Obviously, the optimization problem (8) is convex. We assume it has at least one feasible solution that fulfils constraints (8a)–(8d). Then, at least one optimal solution of (8) exists, and the corresponding optimality conditions can be obtained by using the Karush-Kuhn-Tucker (KKT) conditions based on Theorem 3.34 in [22], and are summarized in the following theorem whose proof is omitted due to space limitations.

Theorem 1. *The feasible solution* $\Delta x_i^*[k+1], \Delta y_i^*[k], \Delta u_i^*[k], \Delta p_{tie_s}^*[k],$ $\forall i \in \mathcal{N}, s \in \mathcal{T}, k \in \mathcal{K}$ *of problem* (8) *is optimal if and only if for any* $k \in \mathcal{K}$, *there exist constants* $\alpha_i^*[k] \in \mathbb{R}^4$, $\beta_i^*[k] \in \mathbb{R}$, $\forall i \in \mathcal{N}_{\mathcal{G}},$ $\alpha_i^*[k], \beta_i^*[k] \in \mathbb{R}^2$, $\forall i \in \mathcal{N}_{\mathcal{L}}$, $\gamma_s^*[k] \in \mathbb{R}$, $\forall s \in \mathcal{T}$, $\lambda_i^*[k], \mu_i^*[k] \in \mathbb{R}_+,$ $\forall i \in \mathcal{N}$ *such that the following conditions hold for all* $i \in \mathcal{N}, s \in \mathcal{T}, k \in \mathcal{K}$

$$
0 \in \mathcal{A}_{x_i}(\Delta x_i^*[k+1] + x_i(hT_o)) + \mathcal{B}_{x_i} + \mathcal{A}_{h_{ii}}^T \alpha_i^*[k+1]
$$
$$
+ \sum_{j \in \mathcal{N}_i} \mathcal{A}_{h_{ij}}^T \alpha_j^*[k+1] - \alpha_i^*[k] + \mathcal{D}_{h_{ii}}^T \beta_i^*[k+1]
$$
$$
+ \sum_{j \in \mathcal{N}_i} \mathcal{D}_{h_{ij}}^T \beta_j^*[k+1] - \mathcal{J}_{m_i}(\lambda_i^*[k] - \lambda_i^*[k+1])
$$
$$
+ \mathcal{J}_{m_i}(\mu_i^*[k] - \mu_i^*[k+1]) + C_{\Omega_{x_i}}(\Delta x_i^*[k+1]) \tag{10a}
$$

$$
0 \in \mathcal{A}_{y_i}(\Delta y_i^*[k] + y_i(hT_o)) + \mathcal{B}_{h_i}^T \alpha_i^*[k] + \mathcal{E}_{h_i}^T \beta_i^*[k]
$$
$$
- \mathcal{J}_{b_i} \gamma_{s_i}^*[k] + C_{\Omega_{y_i}}(\Delta y_i^*[k]) \tag{10b}
$$

$$
0 \in \mathcal{A}_{u_i}(\Delta u_i^*[k] + u_i^-(hT_o)) + \mathcal{B}_{u_i} + C_{h_i}^T \alpha_i^*[k]
$$
$$
+ \mathcal{F}_{h_i}^T \beta_i^*[k] + C_{\Omega_{u_i}}(\Delta u_i^*[k]) \tag{10c}
$$

$$
0 = \mathcal{A}_{tie_s}\left(\Delta p_{tie_s}^*[k] + p_{tie_s}(hT_o) - p_{tie_s}^{ref}\right) + \gamma_s^*[k] \tag{10d}
$$

$$
0 = \lambda_i^*[k](\underline{r}_{m_i} - \mathcal{J}_{m_i}^T(\Delta x_i^*[k+1] - \Delta x_i^*[k])) \tag{10e}
$$

$$
0 = \mu_i^*[k]\left(\mathcal{J}_{m_i}^T(\Delta x_i^*[k+1] - \Delta x_i^*[k]) - \overline{r}_{m_i}\right) \tag{10f}
$$

where s_i *is the index of the control area that bus* i *belongs to;* $\alpha_i^*[n_p] = 0_{4 \times 1},$ $\beta_i^*[n_p] = 0$, $\forall i \in \mathcal{N}_{\mathcal{G}}$; $\alpha_i^*[n_p] = \beta_i^*[n_p] = 0_{2 \times 1}$, $\forall i \in \mathcal{N}_{\mathcal{L}}$; *and*

$$
\lambda_i^*[n_p] = \mu_i^*[n_p] = 0, \forall i \in \mathcal{N}.
$$

4. Distributed solution algorithm

In this section, we propose a projection-based algorithm to solve the MPC problem (8) in a distributed way. To develop the distributed algorithm, we assign each control area a connected communication network whose topology contains all the links of the area in the transmission network. Furthermore, for the control areas that are physically interconnected, we connect those communication networks by adding links with the same ends as the corresponding tie lines. We assume any two cyber-connected buses, i.e., neighbouring buses in the communication network of the entire system, can share information with each other via bidirectional communication.

In our method, for each prediction window $t \in [hT_o, (h+n_p)T_o)$, we introduce four new variables $x_{i(k+1)}, y_{ik}, u_{ik}, v_{ik}$ for each bus $i \in \mathcal{N}$ and time slot $k \in \mathcal{K}$ to compute the optimal solution of the MPC problem (8), where $x_{i(k+1)} \in \mathbb{R}^4$, $y_{ik}, u_{ik}, v_{ik} \in \mathbb{R}$, $\forall i \in \mathcal{N}_{\mathcal{G}}, k \in \mathcal{K}$, and $x_{i(k+1)}, y_{ik} \in \mathbb{R}^2, u_{ik} \in \mathbb{R}^3, v_{ik} \in \mathbb{R}, \forall i \in \mathcal{N}_{\mathcal{L}}, k \in \mathcal{K}$. At each time step $t = hT_o$, bus i implements the designed algorithm to calculate $x_{i(k+1)}, y_{ik},$ u_{ik}, v_{ik} in parallel for all time slots in the prediction window, i.e., $\forall k \in \mathcal{K}$, to solve problem (8). In particular, for each $k \in \mathcal{K}$, bus i runs the following dynamics

$$
\dot{\tilde{x}}_{i(k+1)} = x_{i(k+1)} - \tilde{x}_{i(k+1)} - \mathcal{A}_{x_i}(x_{i(k+1)} + x_i(hT_o)) - \mathcal{B}_{x_i}
$$
$$
+ \mathcal{J}_{m_i}(P_{\mathbb{R}_+}(\lambda_{ik} + \tilde{\lambda}_{ik}) - P_{\mathbb{R}_+}(\lambda_{i(k+1)} + \tilde{\lambda}_{i(k+1)}))
$$
$$
- \mathcal{J}_{m_i}(P_{\mathbb{R}_+}(\mu_{ik} + \tilde{\mu}_{ik}) - P_{\mathbb{R}_+}(\mu_{i(k+1)} + \tilde{\mu}_{i(k+1)}))
$$
$$
+ (\alpha_{ik} + \hat{\alpha}_{ik}) - \mathcal{A}_{h_{ii}}^T(\alpha_{i(k+1)} + \hat{\alpha}_{i(k+1)})
$$
$$
- \sum_{j \in \mathcal{N}_i} \mathcal{A}_{h_{ij}}^T(\alpha_{j(k+1)} + \hat{\alpha}_{j(k+1)})
$$
$$
- \mathcal{D}_{h_{ii}}^T(\beta_{i(k+1)} + \hat{\beta}_{i(k+1)})
$$
$$
- \sum_{j \in \mathcal{N}_i} \mathcal{D}_{h_{ij}}^T(\beta_{j(k+1)} + \hat{\beta}_{j(k+1)}) \tag{11a}
$$

$$
\dot{\tilde{y}}_{ik} = y_{ik} - \tilde{y}_{ik} - \mathcal{A}_{y_i}(y_{ik} + y_i(hT_o)) - \mathcal{B}_{h_i}^T(\alpha_{ik} + \hat{\alpha}_{ik})
$$
$$
- \mathcal{E}_{h_i}^T(\beta_{ik} + \hat{\beta}_{ik}) + \mathcal{J}_{b_i}(\rho_{ik} + \hat{\rho}_{ik}) \tag{11b}
$$

$$
\dot{\tilde{u}}_{ik} = u_{ik} - \tilde{u}_{ik} - \mathcal{A}_{u_i}(u_{ik} + u_i^-(hT_o)) - \mathcal{B}_{u_i}
$$
$$
- C_{h_i}^T(\alpha_{ik} + \hat{\alpha}_{ik}) - \mathcal{F}_{h_i}^T(\beta_{ik} + \hat{\beta}_{ik}) \tag{11c}
$$

$$
\dot{v}_{ik} = - \mathcal{A}_{tie_{s_i}}\left(v_{ik} + p_{b_i}(hT_o) - \mathcal{J}_{t_i} P_{tie_{s_i}}^{ref}\right)
$$
$$
- \frac{1}{n_{s_i}}(\rho_{ik} + \hat{\rho}_{ik}) \tag{11d}
$$

$$
\dot{\alpha}_{ik} = \tilde{\alpha}_{ik}, \quad \dot{\hat{\alpha}}_{ik} = -\hat{\alpha}_{ik} + \tilde{\alpha}_{ik} \tag{11e}
$$

$$
\dot{\beta}_{ik} = \tilde{\beta}_{ik}, \quad \dot{\hat{\beta}}_{ik} = -\hat{\beta}_{ik} + \tilde{\beta}_{ik} \tag{11f}
$$

$$
\dot{\rho}_{ik} = \tilde{\rho}_{ik}, \quad \dot{\hat{\rho}}_{ik} = -\hat{\rho}_{ik} + \tilde{\rho}_{ik} \tag{11g}
$$

$$
\dot{\lambda}_{ik} = P_{\mathbb{R}_+}(\lambda_{ik} + \tilde{\lambda}_{ik}) - \lambda_{ik} \tag{11h}
$$

$$
\dot{\mu}_{ik} = P_{\mathbb{R}_+}(\mu_{ik} + \tilde{\mu}_{ik}) - \mu_{ik} \tag{11i}
$$

$$
\dot{\phi}_{ik} = -\sum_{j \in \tilde{\mathcal{N}}_i}(\rho_{ik} + \hat{\rho}_{ik} - \rho_{jk} - \hat{\rho}_{jk}) \tag{11j}
$$

$$
x_{i(k+1)} = P_{\Omega_{x_i}}(\tilde{x}_{i(k+1)}), \quad y_{ik} = P_{\Omega_{y_i}}(\tilde{y}_{ik}), \quad u_{ik} = P_{\Omega_{u_i}}(\tilde{u}_{ik}) \tag{11k}
$$

where $\alpha_{in_p} = \hat{\alpha}_{in_p} = \tilde{\alpha}_{in_p} = 0_{4 \times 1}$, $\beta_{in_p} = \hat{\beta}_{in_p} = \tilde{\beta}_{in_p} = 0$, $\forall i \in \mathcal{N}_{\mathcal{G}}$; $\alpha_{in_p} = \hat{\alpha}_{in_p} = \tilde{\alpha}_{in_p} = \beta_{in_p} = \hat{\beta}_{in_p} = \tilde{\beta}_{in_p} = 0_{2 \times 1}$, $\forall i \in \mathcal{N}_{\mathcal{L}}$; $\lambda_{in_p} = \tilde{\lambda}_{in_p} = \mu_{in_p} = \tilde{\mu}_{in_p} = 0, \forall i \in \mathcal{N}$; $\tilde{x}_{i(k+1)}, \tilde{y}_{ik}, \tilde{u}_{ik}, v_{ik}, \alpha_{ik}, \hat{\alpha}_{ik}, \beta_{ik}, \hat{\beta}_{ik}, \rho_{ik}, \hat{\rho}_{ik},$ $\lambda_{ik}, \mu_{ik}, \phi_{ik}$ are the state variables with $\tilde{x}_{i(k+1)}, \alpha_{ik}, \hat{\alpha}_{ik} \in \mathbb{R}^4$, $\tilde{y}_{ik}, \hat{u}_{ik},$ $v_{ik}, \beta_{ik}, \hat{\beta}_{ik}, \rho_{ik}, \hat{\rho}_{ik}, \lambda_{ik}, \mu_{ik}, \phi_{ik} \in \mathbb{R}$, $\forall i \in \mathcal{N}_{\mathcal{G}}, k \in \mathcal{K}$, and $\tilde{x}_{i(k+1)},$

$\tilde{y}_{ik}, \alpha_{ik}, \hat{\alpha}_{ik}, \beta_{ik}, \hat{\beta}_{ik} \in \mathbb{R}^2,$ $\quad u_{ik} \in \mathbb{R}^3,$ $\quad v_{ik}, \rho_{ik}, \hat{\rho}_{ik},$ $\quad \lambda_{ik}, \mu_{ik}, \phi_{ik} \in \mathbb{R},$ $\forall i \in \mathcal{N}_{\mathcal{L}}, k \in \mathcal{K};$ and $\tilde{\alpha}_{ik}, \tilde{\beta}_{ik}, \tilde{\rho}_{ik}, \tilde{\lambda}_{ik}, \tilde{\mu}_{ik}$ are the auxiliary variables defined by

$$\tilde{\alpha}_{ik} = \mathcal{A}_{h_{ii}} x_{ik} + \sum_{j \in \mathcal{N}_i} \mathcal{A}_{h_{ij}} x_{jk} + \mathcal{B}_{h_i} y_{ik} + \mathcal{C}_{h_i} u_{ik} - x_{i(k+1)}$$

$$\tilde{\beta}_{ik} = \mathcal{D}_{h_{ii}} x_{ik} + \sum_{j \in \mathcal{N}_i} \mathcal{D}_{h_{ij}} x_{jk} + \mathcal{E}_{h_i} y_{ik} + \mathcal{F}_{h_i} u_{ik} + \mathcal{G}_{h_i} \Delta r_i[k]$$

$$\tilde{\rho}_{ik} = v_{ik} - \mathcal{J}_{b_i}^T y_{ik} + \sum_{j \in \tilde{\mathcal{N}}_i} (\phi_{ik} - \phi_{jk})$$

$$\tilde{\lambda}_{ik} = \underline{r}_{m_i} - \mathcal{J}_{m_i}^T (x_{i(k+1)} - x_{ik})$$

$$\tilde{\mu}_{ik} = \mathcal{J}_{m_i}^T (x_{i(k+1)} - x_{ik}) - \bar{r}_{m_i}.$$

Moreover, $\tilde{\mathcal{N}}_i$ is the index set of buses that are cyber-connected with bus i and locate in the same control area as bus i, and n_s is the number of buses that control area s contains. In (11), we assume that the scheduled net tie-line power $p_{tie_s}^{ref}$ of the sth control area, $s \in \mathcal{T}$, is only known to one bus $i_s \in \mathcal{N}_s$ (bus i_s can be arbitrarily selected). Therefore, $\mathcal{J}_{t_i} \in \mathbb{R}$ in (11d) is defined by $\mathcal{J}_{t_i} = 1$ if $i = i_s$, and $\mathcal{J}_{t_i} = 0$ otherwise. In what follows, we will interchangeably use the terms system (11) or algorithm (11).

As mentioned before, variables $x_{i(k+1)}, y_{ik}, u_{ik}, v_{ik}$ are introduced to compute the optimal solution of problem (8). In fact, let $\tilde{x}_{i(k+1)}^*, \tilde{y}_{ik}^*, \tilde{u}_{ik}^*,$ $x_{i(k+1)}^*, y_{ik}^*, u_{ik}^*, v_{ik}^*, \alpha_{ik}^*, \hat{\alpha}_{ik}^*, \beta_{ik}^*, \hat{\beta}_{ik}^*, \rho_{ik}^*, \hat{\rho}_{ik}^*, \lambda_{ik}^*, \mu_{ik}^*, \phi_{ik}^*, \forall i \in \mathcal{N}, k \in \mathcal{K}$ be an equilibrium point of (11), then we claim that $x_{i(k+1)}^*, y_{ik}^*, u_{ik}^*, p_{tie_s k}^*$ with $p_{tie_s k}^* = \sum_{i \in \mathcal{N}_s} v_{ik}^*, \forall s \in \mathcal{T}$ satisfy the feasibility conditions (8a)-(8d) and optimality conditions (10a)-(10f) for all $i \in \mathcal{N}, s \in \mathcal{T}, k \in \mathcal{K}$, and therefore yield an optimal solution of the MPC problem (8).

Firstly, note that at the steady state $\dot{\alpha}_{ik} = 0, \dot{\beta}_{ik} = 0$, the feasibility condition (8a) is satisfied based on the definitions of auxiliary variables $\tilde{\alpha}_{ik}$ and $\tilde{\beta}_{ik}$. Thus, Eqs. (11e), (11f) are used to enforce the prediction constraint (8a). Further, if $\dot{\lambda}_{ik} = \dot{\mu}_{ik} = 0$, the following two equations hold

$$\lambda_{ik}^* = \mathrm{P}_{\mathbb{R}_+}(\lambda_{ik}^* + \underline{r}_{m_i} - \mathcal{J}_{m_i}^T(x_{i(k+1)}^* - x_{ik}^*))$$

$$\mu_{ik}^* = \mathrm{P}_{\mathbb{R}_+}(\mu_{ik}^* + \mathcal{J}_{m_i}^T(x_{i(k+1)}^* - x_{ik}^*) - \bar{r}_{m_i}). \tag{12}$$

According to Lemma 4.1 in [23], for any $\xi, \eta \in \mathbb{R}, \xi = \mathrm{P}_{\mathbb{R}_+}(\xi + \eta)$ if and only if $\xi \geq 0, \eta \leq 0,$ and $\xi\eta = 0$. Therefore, it follows from (12) that

$$\lambda_{ik}^* \geq 0, \ \mu_{ik}^* \geq 0$$

$$\bar{r}_{m_i} \geq \mathcal{J}_{m_i}^T(x_{i(k+1)}^* - x_{ik}^*) \geq \underline{r}_{m_i}$$

$$\lambda_{ik}^*(\underline{r}_{m_i} - \mathcal{J}_{m_i}^T(x_{i(k+1)}^* - x_{ik}^*)) = 0$$

$$\mu_{ik}^*(\mathcal{J}_{m_i}^T(x_{i(k+1)}^* - x_{ik}^*) - \bar{r}_{m_i}) = 0 \tag{13}$$

for all $i \in \mathcal{N}, k \in \mathcal{K}$, which suggests that Eqs. (11h), (11i) are designed to enforce conditions (8b), (10e), (10f), i.e., the constraints and optimality conditions related to the ramping rates of generators.

At the equilibrium point, $\dot{\rho}_{ik} = \dot{\hat{\rho}}_{ik} = 0$ gives $\hat{\rho}_{ik} = \tilde{\rho}_{ik} = 0$. Then, $\dot{v}_{ik} = 0$ and $\dot{\phi}_{ik} = 0$ with $\hat{\rho}_{ik} = \tilde{\rho}_{ik} = 0$ indicate

$$\sum_{j \in \tilde{\mathcal{N}}_i} (\rho_{ik}^* - \rho_{jk}^*) = 0 \tag{14a}$$

$$\mathcal{A}_{tie_s}\left(v_{ik}^* + p_{b_i}(hT_o) - \mathcal{J}_{t_i} p_{tie_{s_i}}^{ref}\right) + \frac{1}{n_{s_i}}\rho_{ik}^* = 0 \tag{14b}$$

$$v_{ik}^* - \mathcal{J}_{b_i}^T y_{ik}^* + \sum_{j \in \tilde{\mathcal{N}}_i} (\phi_{ik}^* - \phi_{jk}^*) = 0 \tag{14c}$$

for all $i \in \mathcal{N}, k \in \mathcal{K}$. Since the topology of the communication network for each control area is connected, (14a) implies that ρ_{ik}^* is identical for all buses within the same control area [3]. Without loss of generality, for the sth control area, $s \in \mathcal{T}$, we let $\rho_{ik}^* = \varsigma_{sk}^*, \forall i \in \mathcal{N}_s$. Then, by summing up Eq. (14b) for all buses within the sth control area, we have

$$\mathcal{A}_{tie}\left(\sum_{i \in \mathcal{N}_s} v_{ik}^* + p_{tie_s}(hT_o) - p_{tie_s}^{ref}\right) + \varsigma_{sk}^* = 0 \tag{15}$$

for all $s \in \mathcal{T}, k \in \mathcal{K}$. Similarly, summing up (14c) for all buses that

belong to the sth control area gives

$$\sum_{i \in \mathcal{N}_s} v_{ik}^* = \sum_{i \in \mathcal{N}_s} \mathcal{J}_{b_i}^T y_{ik}^*, \ \forall i \in \mathcal{N}, k \in \mathcal{K}. \tag{16}$$

Combining (15) and (16) gives that the equilibrium point of system (11) satisfies conditions (8d) and (10d) with $p_{tie_s k}^* = \sum_{i \in \mathcal{N}_s} v_{ik}^*,$ $\forall s \in \mathcal{T}, k \in \mathcal{K}$. Therefore, Eqs. (11d), (11g) and (11j) are designed to achieve the feasibility and optimality conditions with respect to the net inter-area power exchanges.

Let $\dot{\tilde{u}}_{ik} = 0$, then we have

$$\tilde{u}_{ik}^* = u_{ik}^* - \mathcal{A}_{u_i}(u_{ik}^* + u_i^-(hT_o)) - \mathcal{B}_{u_i} - C_{h_i}^T \alpha_{ik}^* - \mathcal{F}_{h_i}^T \beta_{ik}^* \tag{17}$$

for all $i \in \mathcal{N}, k \in \mathcal{K}$ at the steady state, where we use the facts $\hat{\alpha}_{ik}^* = 0,$ $\hat{\beta}_{ik}^* = 0$ from $\dot{\alpha}_{ik} = \dot{\hat{\alpha}}_{ik} = 0$ and $\dot{\beta}_{ik} = \dot{\hat{\beta}}_{ik} = 0$ to get Eq. (17). Applying the projection operator $\mathrm{P}_{\Omega_{u_i}}(\cdot)$ on both sides of (17), we have

$$u_{ik}^* = \mathrm{P}_{\Omega_{u_i}}(\tilde{u}_{ik}^*) = \mathrm{P}_{\Omega_{u_i}}(u_{ik}^* - \mathcal{A}_{u_i}(u_{ik}^* + u_i^-(hT_o))$$
$$- \mathcal{B}_{u_i} - C_{h_i}^T \alpha_{ik}^* - \mathcal{F}_{h_i}^T \beta_{ik}^*) \tag{18}$$

for all $i \in \mathcal{N}, k \in \mathcal{K}$, where we notice that $u_{ik}^* = \mathrm{P}_{\Omega_{u_i}}(\tilde{u}_{ik}^*)$ from (11k). Then, according to the definition of normal cone, the following fact holds

$$0 \in \mathcal{A}_{u_i}(u_{ik}^* + u_i^-(hT_o)) + \mathcal{B}_{u_i} + C_{h_i}^T \alpha_{ik}^*$$
$$+ \mathcal{F}_{h_i}^T \beta_{ik}^* + \mathcal{C}_{\Omega_{u_i}}(u_{ik}^*), \ \forall i \in \mathcal{N}, k \in \mathcal{K}. \tag{19}$$

Hence, the equilibrium point of (11) fulfils condition (10c). By following the similar arguments as for deriving (19), we have conditions (10a), (10b) are satisfied at the steady state from $\dot{x}_{i(k+1)} = 0, \dot{y}_{ik} = 0$. Consequently, Eqs. (11a)-(11c) are introduced to enforce the optimality conditions (10a)-(10c).

Finally, Eq. (11k) makes variables $x_{i(k+1)}^*, y_{ik}^*, u_{ik}^*, \forall i \in \mathcal{N}, k \in \mathcal{K}$ fulfil the feasibility constraint (8c) by projecting their unconstrained counterparts $\tilde{x}_{i(k+1)}^*, \tilde{y}_{ik}^*, \tilde{u}_{ik}^*$ into the corresponding admissible ranges.

Now, we have shown that $x_{i(k+1)}^*, \ y_{ik}^*, \ u_{ik}^*, \ p_{tie_s k}^*,$ $\forall i \in \mathcal{N}, s \in \mathcal{T}, k \in \mathcal{K}$ fulfil constraints (8a)-(8d) and the optimality conditions (10a)-(10f) of the MPC problem (8), which hence gives rise to the following Theorem

Theorem 2. *At the equilibrium point of system* (11), $x_{i(k+1)}^*, y_{ik}^*, u_{ik}^*, p_{tie_s k}^*$ *with* $\hat{p}_{tie_s k}^* = \sum_{i \in \mathcal{N}_s} v_{ik}^*, \forall i \in \mathcal{N}, s \in \mathcal{T}, k \in \mathcal{K}$ *is an optimal solution of the MPC problem* (8)*.*

Theorem 3 establishes the asymptotic convergence of algorithm (11)*, whose proof is omitted due to space limitations.*

Theorem 3. *Given any bounded initial conditions, the trajectories of system* (11) *are bounded and asymptotically converge to an equilibrium point, namely, algorithm* (11) *asymptotically converges to an optimal solution of the MPC problem* (8)*.*

It should be pointed out that the dynamics at each bus $i \in \mathcal{N}$ in system (11) only relies on local information and information pertaining to $\alpha_{jk}, \hat{\alpha}_{jk}, \beta_{jk}, \hat{\beta}_{jk}, \rho_{jk}, \hat{\rho}_{jk}, \phi_{jk}, \forall k \in \mathcal{K}$, received from its cyber-connected buses. Therefore, algorithm (11) can be implemented in a fully distributed way.

Remark 1. For simplicity, we neglect the computational time of using the designed projection-based algorithm (11) to solve the MPC problem (8) at each sampling instant $t = hT_o, h \in \mathbb{Z}_+$. Nevertheless, it inevitably requires a certain period of time for (11) to achieve convergence in practice, which may impose negative impacts on the frequency regulation performance of the proposed control method. Furthermore, compared with the traditional AGC, our method may incur a heavy computation burden in total. However, because the proposed method is fully distributed, the computation burden is decomposed into each bus. Of course, it is still of importance to consider these issues in the design process, which will be studied in the future.
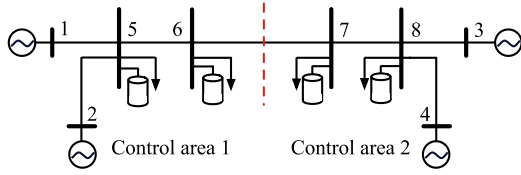
Fig. 1. Diagram for the 8-bus test system.

5. Case studies

In this section, the effectiveness and efficiency of the proposed DMPC-based frequency control algorithm is tested on an 8-bus power system in which we add 4 energy storage devices at buses 5–8, respectively. The diagram of the test system is shown in Fig. 1, where the system is divided into two control areas by the red dashed line. The system parameters with respect to generator buses, load buses and transmission lines that are in per unit on a base of 100 MW are presented in Table 1. We assume that each generator has the identical power limits $\underline{p}_{m_i} = 0$, $\bar{p}_{m_i} = 0.5$ p.u., and ramping limits $\underline{r}_{m_i} = -0.24$ p.u./min, $\bar{r}_{m_i} = 0.3$ p.u./min; each controllable load has the same bounds on its power consumption $\underline{p}_{l_i} = 0$, $\bar{p}_{l_i} = 0.4$ p.u.; each energy storage device is subject to the same power limits $\bar{p}_{c_i} = \bar{p}_{d_i} = 0.2$ p.u., and energy capacity constraints $\underline{e}_i = 0$, $\bar{e}_i = 1$ p.u. · min. Furthermore, we set the charging/discharging efficiencies as $\eta_{c_i} = \eta_{d_i} = 1$, and initial energy level as $e_i(t_0) = 0.3$ p.u. · min for all storage units. The amplitude constraints on bus frequency deviations are -4×10^{-3} p.u. and 4×10^{-3} p.u. The sampling period and prediction step for the MPC problem are set to be $h = 0.5$ s and $n_p = 8$, respectively.

The time-varying net demand disturbances shown in Fig. 2 are applied to the load buses. For brevity, we assume that no prediction errors exist. In this case, we compare the control performance between the DMPC-based frequency controller and AGC, where AGC is implemented as in [2] with the integral gain for each control area's area control error (ACE) being 0.1 and the participation factor for each generator being proportional to a_{m_i}. To guarantee a desirable transient control performance of AGC, we set the frequency-bias coefficient for the ACE signal of each control area as $\sigma_s = \sum_{i \in \mathcal{N}_s} (D_i + \frac{1}{R_i})$, $s = 1, 2$ [2]. Fig. 3 gives the state responses of the area-wise frequency and net inter-area power exchange deviations from the nominal values under different control methods, where the frequency of each control area is synthesized by adopting the well-known concept of center of inertia (CoI) [24]. It can be observed that the system frequency can be constrained within the acceptable range by the DMPC-based frequency controller, and a better control performance can also be achieved.

To illustrate that the power capacity limits of all controllable units are satisfied by our method at any time, we take the active power contributions of the synchronous generator at bus 1 and controllable load as well as energy storage device at bus 5 for instance, which are

Fig. 2. Net demand profiles for load buses.
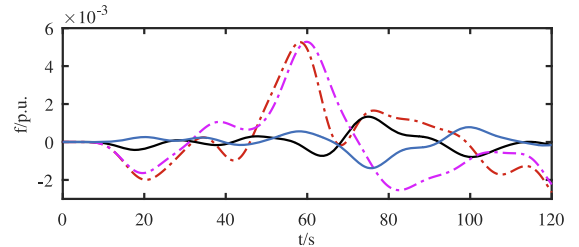
(a) Frequency responses (the DMPC-based method: black solid line (area 1) and blue solid line (area 2); AGC: red dashed line (area 1) and pink dashed line (area 2)
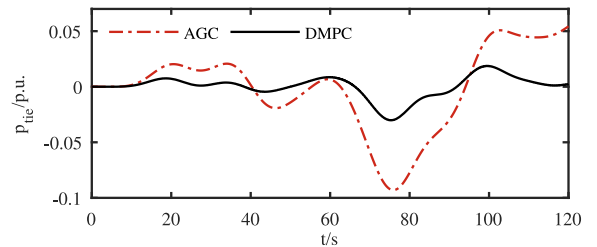
(b) Net Power flows from bus 6 to bus 7

Fig. 3. State responses of the system.

presented in Fig 4. The stored energy levels of all storage units are given in Fig 5. Obviously, the storage energy constraints are fulfilled all the time.

6. Conclusion

This paper has investigated frequency regulation of multi-area power systems by adopting a distributed model predictive control algorithm that can regulate the system frequency and net tie-line power flows between interconnected control areas. The frequency regulation task has been firstly formulated as a constrained MPC problem, and then a distributed projection-based algorithm has been proposed to solve the resulting optimization problem. Case studies have verified the performance of the designed controller.

Table 1
Parameters of the test system.

	1	2	3	4	5	6	7	8
M_i	13	13	12.35	12.35	-	-	-	-
D_i	1	0.8	1.1	1	0.9	1	1.2	0.8
T_{m_i}	1.2	0.8	0.9	1	-	-	-	-
T_{v_i}	0.3	0.4	0.35	0.3	-	-	-	-
R_i	0.05	0.05	0.05	0.05	-	-	-	-
$a_{m_i}(a_{l_i})$	0.35	0.37	0.89	0.78	0.48	0.35	0.67	0.56
$b_{m_i}(b_{l_i})$	-0.14	-0.81	-0.27	-1.79	0.15	0.11	0.27	0.12
$c_{m_i}(c_{l_i})$	5.4	7.2	3.8	3.6	5.1	4	4.9	6.2
b_{cd_i}	-	-	-	-	0.096	0.135	0.097	0.086
c_{cd_i}	-	-	-	-	1.3	0.9	2.1	1.8
B_{ij}	$B_{15} = 11.11$, $B_{25} = 6.67$, $B_{38} = 11.11$, $B_{48} = 6.67$, $B_{56} = 11.11$, $B_{67} = 9.09$, $B_{78} = 11.11$							
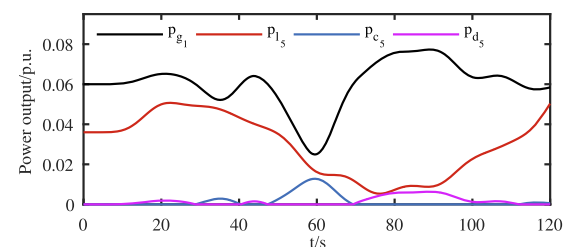
Fig. 4. Power outputs of the synchronous generator at bus 1, energy storage device at bus 5 and controllable load at bus 5.
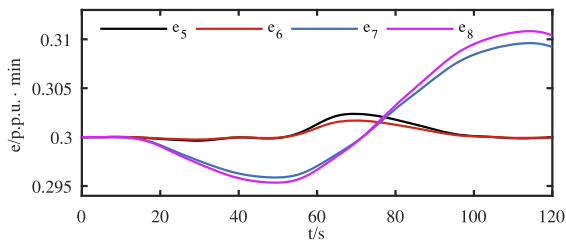
Fig. 5. Energy levels of storage devices.

Declaration of Competing Interest

The authors declare that they have no known competing financial interests or personal relationships that could have appeared to influence the work reported in this paper.

Acknowledgement

References

[1] C. Zhao, E. Mallada, S.H. Low, J. Bialek, Distributed plug-and-play optimal generator and load control for power system frequency regulation, Int. J. Electr. Power Energy Syst. 101 (2018) 1–12.

[2] P. Kundur, Power System Stability and Control, McGraw-Hill, New York, 1994.

[3] T. Liu, D.J. Hill, C. Zhang, Non-disruptive load-side control for frequency regulation in power systems, IEEE Trans. Smart Grid 7 (4) (2016) 2142–2153.

[4] L. Yang, T. Liu, D.J. Hill, Distributed optimization for multi-time slot economic dispatch, Proc. IEEE PES Gen. Meeting, Atlanta, GA, USA, (2019), pp. 1–5.

[5] C. Zhao, U. Topcu, N. Li, S.H. Low, Design and stability of load- side primary frequency control in power systems, IEEE Trans. Autom. Control 59 (5) (2014) 1177–1189.

[6] C. Zhang, Y. Xu, Z.Y. Dong, J. Ma, Robust operation of microgrids via two-stage coordinated energy storage and direct load control, IEEE Trans. Power Syst. 32 (4) (2017) 2858–2868.

[7] R. Lu, S.H. Hong, M. Yu, Demand response for home energy management using reinforcement learning and artificial neural network, IEEE Trans. Smart Grid 10 (6) (2019) 6629–6639.

[8] A. Attarha, N. Amjady, S. Dehghan, B. Vatani, Adaptive robust self-scheduling for a wind producer with compressed air energy storage, IEEE Trans. Sustain. Energy 9 (4) (2018) 1659–1671.

[9] S.K. Pandey, S.R. Mohanty, N. Kishor, A literature survey on load-frequency control for conventional and distribution generation power systems, Renew. Sustain. Energy Rev. 25 (2013) 318–334.

[10] H. Jiang, J. Lin, Y. Song, D.J. Hill, MPC-based frequency control with demand-side participation: a case study in an isolated wind-aluminum power system, IEEE Trans. Power Syst. 30 (6) (2015) 3327–3337.

[11] A.M. Ersdal, L. Imsland, K. Uhlen, Model predictive load-frequency control, IEEE Trans. Power Syst. 31 (1) (2015) 777–785.

[12] P. McNamara, F. Milano, Model predictive control-based AGC for multi-terminal HVDC-connected AC grids, IEEE Trans. Power Syst. 33 (1) (2017) 1036–1048.

[13] A.N. Venkat, I.A. Hiskens, J.B. Rawlings, S.J. Wright, Distributed MPC strategies with application to power system automatic generation control, IEEE Trans. Control Syst. Technol. 16 (6) (2008) 1192–1206.

[14] X. Liu, Y. Zhang, K.Y. Lee, Coordinated distributed MPC for load frequency control of power system with wind farms, IEEE Trans. Ind. Informat. 64 (6) (2016) 5140–5150.

[15] K. Baker, J. Guo, G. Hug, X. Li, Distributed MPC for efficient coordination of storage and renewable energy sources across control areas, IEEE Trans. Smart Grid 7 (2) (2016) 992–1001.

[16] K. Worthmann, C.M. Kellett, P. Braun, L. Grüne, S.R. Weller, Distributed and decentralized control of residential energy systems incorporating battery storage, IEEE Trans. Smart Grid 6 (4) (2015) 1914–1923.

[17] G.K. Larsen, N.D. Van Foreest, J.M. Scherpen, Distributed MPC applied to a network of households with micro-CHP and heat storage, IEEE Trans. Smart Grid 5 (4) (2014) 2106–2114.

[18] A.R. Bergen, D.J. Hill, A structure preserving model for power system stability analysis, IEEE Trans. Power App. Syst. PAS-100 (1) (1981) 25–35.

[19] M. Larsson, D.J. Hill, G. Olsson, Emergency voltage control using search and predictive control, Int. J. Elect. Power Energy Syst. 24 (2) (2002) 121–130.

[20] S. Trip, C. De Persis, Distributed optimal load frequency control with non-passive dynamics, IEEE Trans. Control Netw. Syst. 5 (3) (2017) 1232–1244.

[21] Y. Zheng, D.J. Hill, Z.Y. Dong, Multi-agent optimal allocation of energy storage systems in distribution systems, IEEE Trans. Sustain. Energy 8 (4) (2017) 1715–1725.

[22] A.P. Ruszczyński, Nonlinear Optimization, Princeton university press, 2006.

[23] S. Yang, Q. Liu, J. Wang, A multi-agent system with a proportional-integral protocol for distributed constrained optimization, IEEE Trans. Autom. Control 62 (7) (2017) 3461–3467.

[24] F. Milano, Rotor speed-free estimation of the frequency of the center of inertia, IEEE Trans. Power Syst. 33 (1) (2018) 1153–1155.